# Direct Extraction of the Series Equivalent Circuit Parameters for the Small-Signal Model of SOI MOSFET's

J. P. Raskin, *Member, IEEE*, G. Dambrine, *Member, IEEE*, and R. Gillon, *Member, IEEE*

***Abstract*—A new extraction scheme is proposed which allows to determine all the series equivalent circuit elements values from $S$-parameters measurements at a single bias point in saturation. Exploiting the specific shape of a set of impedance loci, the new scheme uses linear regression techniques to solve the extraction problem. The resulting algorithm is very simple and efficient when compared to optimizer-driven approaches.**

***Index Terms*—FET's, MOSFET, parameter extraction, scattering parameters measurement, small-signal equivalent circuit.**

## I. INTRODUCTION

THE maturation of low-cost silicon-on-insulator (SOI) MOSFET technology in the microwave domain has brought about a need to develop adequate characterization techniques [1]. This is particularly the case for the direct extraction of small-signal equivalent circuits from $S$-parameters. Indeed, methods developed for MESFET's and HEMT's, such as the "cold-FET" method of Dambrine *et al.* [2], are not directly applicable to MOSFET's, because these methods exploit unique features of their specific field-effect transistor (FET) technology [3]. Recently, Lee *et al.* [4] proposed an innovative approach to the extraction problem for bulk MOSFET's. By fitting the frequency evolution of the measured $Z$-parameters with analytic expressions, these authors determine the series elements of the equivalent circuit. Then, after removal of the series elements, all other circuit parameters can be obtained in a manner described by [3]. In the present letter, a new fully analytic technique is proposed for the direct extraction of the series circuit parameters. An original formulation of the extraction problem is introduced, which allows to use linear regression methods instead of a general purpose optimizer as in [4]. The result is a very simple and efficient extraction scheme which only requires $S$-parameters measurements at one bias point in saturation.

Manuscript received August 1, 1997. This work was funded by the "Communauté française" through its program "Actions de recherche concertées," by the "Région Wallonne," and by the ESPRIT program of the European Community.

J. P. Raskin and R. Gillon are with the Laboratoire d'Hyperfréquences, Université Catholique de Louvain (UCL), B-1348 Louvain-la-Neuve, Belgium.

G. Dambrine is with the Département Hyperfréquences et Semiconducteurs, Institut d'Electronique et de Microélectronique du Nord (IEMN), F-59652 Villeneuve d'Ascq Cedex, France.

Publisher Item Identifier S 1051-8207(97)08974-5.

## II. EXTRACTION METHOD

Thin-film SOI MOSFET's were fabricated on low-resistivity P-type SIMOX wafers, using a CMOS-compatible process. The MOSFET's are embedded in a coplanar waveguide structure designed to minimize the ground inductance. Using standards implemented on the SOI wafer, a Through-Reflect-Line (TRL) calibration is performed according to the algorithm of [5]. As a result, the reference planes of the scattering parameters measurements are positioned close to the devices, effectively reducing the input and output shunt parasitic admittances. To allow accurate conversion of $S$-parameters to $Y$- or $Z$-parameters, the reference impedance of the calibration is determined using the method of [6].

Fig. 1 shows the model used for the common-source SOI MOSFET. To evaluate the residual input and output shunt admittances $Y_{\rm rg}$ and $Y_{\rm rd}$, the transistors are biased in deep depletion at $V_{\rm DS} = 0$. In these biasing conditions, the measured admittance matrix $\mathbf{Y}_\mu$ scales almost linearly with respect to the device width $W$ so that $Y_{\rm rg}$ and $Y_{\rm rd}$ can be accurately estimated by extrapolating $Y$-parameter data from a set of transistors with various widths to $W = 0$. After correction of the residual shunt admittances, the $Z$-matrix of the circuit takes the following form:

$$\mathbf{Z}_{\sigma\pi} \hat{=} [\mathbf{Y}_\mu - \mathbf{Y}_\rho]^{-1} = \mathbf{Z}_\sigma + \mathbf{Y}_\pi^{-1} \tag{1}$$

$$\mathbf{Y}_\rho = \begin{bmatrix} Y_{\rm rg} & 0 \\ 0 & Y_{\rm rd} \end{bmatrix} \tag{2}$$

$$\mathbf{Z}_\sigma = \begin{bmatrix} R_{\rm g} + R_{\rm s} & R_{\rm s} \\ R_{\rm s} & R_{\rm d} + R_{\rm s} \end{bmatrix} + j\omega \begin{bmatrix} L_{\rm g} + L_{\rm s} & L_{\rm s} \\ L_{\rm s} & L_{\rm d} + L_{\rm s} \end{bmatrix} \tag{3}$$

$$\mathbf{Y}_\pi = \begin{bmatrix} j\omega(C_{\rm gs} + C_{\rm gd}) & -j\omega C_{\rm gd} \\ G_{m0}e^{-j\omega t} - j\omega C_{\rm gd} & G_{\rm ds} + j\omega(C_{\rm ds} + C_{\rm gd}) \end{bmatrix}. \tag{4}$$

In agreement with the work of Lee *et al.* [4], analytical expressions of the $Z$-parameters are derived which reveal the specific frequency behavior of (1):

$$\mathrm{Re}\,(Z_{\sigma\pi ij}) = \mathrm{Re}\,(Z_{\sigma ij}) + \frac{A_{ij}}{\omega^2 + B,} \qquad \text{for } i, j \in 1, 2 \tag{5}$$

$$\frac{1}{\omega} \cdot \mathrm{Im}\,(Z_{\sigma\pi ij}) = \frac{1}{\omega} \cdot \mathrm{Im}\,(Z_{\sigma ij}) - \frac{E_{ij}}{\omega^2 + B} - \frac{F_{ij}}{\omega^2 \cdot (\omega^2 + B)} \quad \text{for } i, j \in 1, 2 \tag{6}$$

where $B$, the $A_{ij}$, $E_{ij}$, and $F_{ij}$ are real and frequency independent expressions involving only elements contributing to

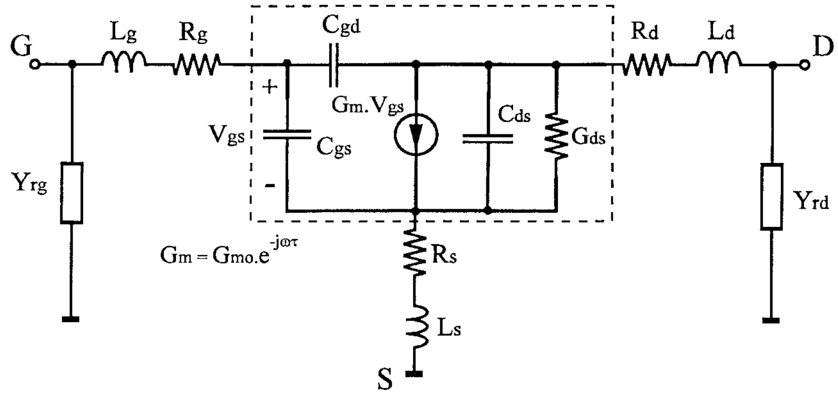


Fig. 1. Small-signal equivalent circuit model for a common-source SOI MOSFET.

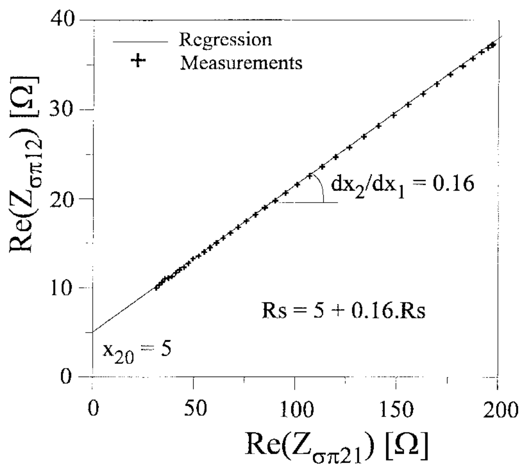


Fig. 2. Parametric plot of resistances in the 0.5–40-GHz band for a conditions for a nMOSFET with $W = 240$ $\mu$m and $L_{\rm eff} = 0.5$ $\mu$m at $V_{\rm GS} = 1$ V and $V_{\rm DS} = 2$ V.

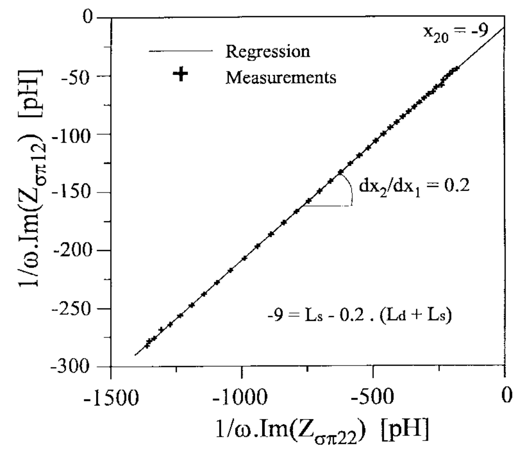


Fig. 3. Parametric plot of inductances in the 0.5–40-GHz band for a conditions for a nMOSFET with $W = 240$ $\mu$m and $L_{\rm eff} = 0.5$ $\mu$m at $V_{\rm GS} = 1$ V and $V_{\rm DS} = 2$ V.

$\mathbf{Y}_\pi$. $F_{12}$ and $F_{22}$ are equal to zero. All series resistances and inductances can thus be obtained from the asymptotic values taken by (5) and (6) at infinite frequency. In order to evaluate these asymptotic values, the authors of [4] use an optimizer to fit the expressions on the right-hand side of (5) and (6) individually to the evolutions of measured data over the available frequency band. It is, however, possible to transform the determination of the asymptotic values into simple linear regression problems.

In the case of the series resistors, this is done by considering the parametric curves defined in a two dimensional plane $[x_1, x_2]$ by $[\mathrm{Re}\,(Z_{\sigma\pi ij}(\omega)), \mathrm{Re}\,(Z_{\sigma\pi kl}(\omega))]$, where $\{i, j\} \neq \{k, l\}$. Using (5), it is straightforward to establish that these curves must be straight lines, and that their intercept at the origin $[0, x_{20}]$ and slope $dx_2/dx_1$ is given by

$$x_{20} = \mathrm{Re}\,(Z_{\sigma kl}) - \frac{A_{kl}}{A_{ij}} \cdot \mathrm{Re}\,(Z_{\sigma_{ij}}), \quad \frac{dx_2}{dx_1} = \frac{A_{kl}}{A_{ij}}. \quad (7)$$

Substituting the values of the intercept and the slope obtained from a linear regression on the measured data points into (7) yields a linear equation relating the series resistances. To determine all series resistances, it is necessary to combine three linearly independent equations formed by varying the indexes $i, j, k, l$ in (7). Such a set of equations can only be constructed when $Z_{\sigma\pi 12}$ and $Z_{\sigma\pi 21}$ are significantly different, which requires to use measurements from the MOSFET in saturation. A sensitivity analysis showed that the following pairs yield the most accurate results: $[\mathrm{Re}\,(Z_{\sigma\pi 11}), \mathrm{Re}\,(Z_{\sigma\pi 21})]$, $[\mathrm{Re}\,(Z_{\sigma\pi 12}), \mathrm{Re}\,(Z_{\sigma\pi 21})]$, $[\mathrm{Re}\,(Z_{\sigma\pi 22}), \mathrm{Re}\,(Z_{\sigma\pi 12})]$. Fig. 2 illustrates the quality of the linear regressions performed on data measured from 500 MHz to 40 GHz. For the series inductances the situation is a little different, because of the more complicated frequency behavior of the right-hand side in (6), when $j = 1$. As can be seen in Fig. 3, the pair $[\mathrm{Im}\,(Z_{\sigma\pi 22})/\omega, \mathrm{Im}\,(Z_{\sigma\pi 12})/\omega]$ produces one useful equation based on the following relations:

$$x_{20} = L_{\rm s} - \frac{E_{12}}{E_{22}} \cdot (L_{\rm d} + L_{\rm s}), \quad \frac{dx_2}{dx_1} = \frac{E_{12}}{E_{22}}. \quad (8)$$

A second equation can be obtained by considering the parametric curve defined in the tridimensional space $[x_1, x_2, x_3]$ by $[\mathrm{Im}\,(Z_{\sigma\pi 21})/\omega, \mathrm{Im}\,(Z_{\sigma\pi 12})/\omega, \mathrm{Im}\,(Z_{\sigma\pi 11})/\omega]$ measured on the saturated MOSFET. Equation (6) imposes that this curve is contained in a plane, of which the intercept at the origin $[0, 0, x_{30}]$ and the slope coefficients $dx_3/dx_1$ and $dx_3/dx_2$

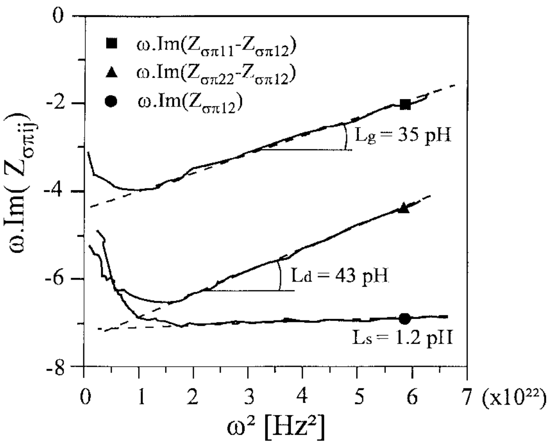


Fig. 4. Extraction of the series inductances in depletion at $V_{\rm GS} = -1$ V and $V_{\rm DS} = 0$ V for a nMOSFET with $W = 240$ $\mu$m and $L_{\rm eff} = 0.5$ $\mu$m.

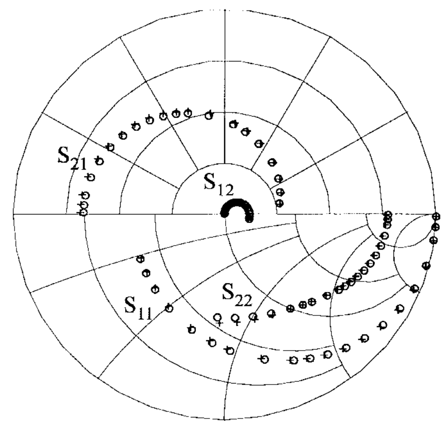


Fig. 5. Measured (o) and modeled (+) $S$-parameters from 0.5 to 40 GHz for a nMOSFET with $W = 240$ $\mu$m and $L_{\rm eff} = 0.5$ $\mu$m, at $V_{\rm GS} = 1$ V and $V_{\rm DS} = 2$ V. $L_{\rm g} = 36$ pH, $L_{\rm d} = 44$ pH, $L_{\rm s} = 0$ pH, $R_{\rm g} = 12.6$ $\Omega$, $R_{\rm d} = 4.2$ $\Omega$, $R_{\rm s} = 5.9$ $\Omega$, $C_{\rm gs} = 150$ fF, $C_{\rm gd} = 40$ fF, $C_{\rm ds} = 37$ fF, $G_{\rm mo} = 17$ mS, $G_{\rm ds} = 2.9$ mS, $\tau = 2$ ps.

can be determined from a linear regression on the measured data:

$$x_{30} = L_{\rm g} + L_{\rm s}\left[1 - \frac{F_{11}}{F_{21}} - \left(\frac{E_{11}}{E_{12}} - \frac{F_{11}E_{21}}{F_{21}E_{12}}\right)\right],$$
$$\frac{dx_3}{dx_1} = \frac{F_{11}}{F_{21}}, \quad \frac{dx_3}{dx_2} = \frac{E_{11}}{E_{12}} - \frac{F_{11}E_{21}}{F_{21}E_{12}}. \tag{9}$$

At this point, it is not possible to combine the measured curves to produce a third linearly independent equation to form a fully determined set of equations. However, as illustrated in Fig. 4, extractions of the series inductances performed on depleted transistors by identifying the square pulsation term in $(\omega Z_{\sigma\pi ij})$ showed that, due to the layout design, $L_{\rm s}$ is negligible with respect to $L_{\rm d}$ and $L_{\rm g}$, being at least 30 times smaller. Accordingly, the third equation used for the evaluation of the inductances is simply: $L_{\rm s} = 0$.

The main advantage of the method based on the parametric curves with respect to the optimization of [4] is that decreasing the device size does not compromise accuracy. Indeed, (7)–(9) are not influenced by the device size, as it cancels out in the ratios $A_{ij}/A_{kl}$, $E_{ij}/E_{kl}$, and $F_{ij}/F_{kl}$. The optimization criteria used by Lee are, on the contrary, based on (5)and (6), where the $A_{ij}$, $E_{ij}$, and $F_{ij}$ terms tend to mask the influence of the series elements in the case of small devices. Other important features of the present method are that it takes advantage of the disymmetry $Z_{\sigma\pi}$ to enhance accuracy, and also that the shared frequency dependence of the $Z_{\sigma\pi ij}$ is correctly and coherently accounted for during the extraction. This latter alleviates the need to discard data below a certain frequency during the extraction of $L_{\rm g}$ [4]. The new extraction scheme has been successfully applied to both enhancement-mode N-channel and accumulation-mode P-channel SOI MOSFET's of various sizes, even for small gate widths. Fig. 5 shows the good match which is typically obtained between the measured $S$-parameter curves and the simulations based on the extracted circuit-parameters, up to 40 GHz.

## III. Conclusion

A new extraction scheme has been demonstrated which, after correction of the residual shunt admittances, allows to determine all the circuit elements values from $S$-parameters measurements at a single bias point in saturation. By splitting the extraction into simple linear regression problems, the new scheme manages to achieve high efficiency and accuracy at the cost of very little sophistication. It is thus well suited for implementation as a fully automatic routine. It also proved to be particularly convenient for the extraction of GaAs MESFET circuit parameters, as it alleviates the need to make forward-biased gate measurements.

## Acknowledgment

The authors wish to thank A. Crahay, B. Katschmarskyj, P. Loumaye, D. Spote, and H. Sablain for device processing.

## References

[1] J. P. Colinge, J. Chen, D. Flandre, J. P. Raskin, R. Gillon, and D. Vanhoenacker, "A low-voltage, low-power microwave SOI MOSFET," in *Proc. 1996 IEEE Int. SOI Conf.,* Fort Myers, FL, Oct. 1996, pp. 128–129.

[2] G. Dambrine, A. Cappy, F. Heliodore, and E. Playez, "A new method for determining the FET small-signal equivalent circuit," *IEEE Trans. Microwave Theory Tech.*, vol. 36, no. 7, pp. 1151–1159, July 1988.

[3] D. Lovelace, J. Costa, and N. Camilleri, "Extracting small-signal model parameters of silicon MOSFET transistors," in *IEEE MTT-S Int. Microwave Symp. Dig.,* 1994, pp. 865–866.

[4] S. Lee, H. K. Yu, C. S. Kim, J. G. Koo, and K. S. Nam, "A novel approach to extracting small-signal model parameters of silicon MOSFET's," *IEEE Microwave Guided Wave Lett.,* vol. 7, no. 3, pp. 75–77, Mar. 1997.

[5] G. F. Engen and C. A. Hoer, "Thru-reflect-line: An improved technique for calibrating the dual six-port automatic network analyzer," *IEEE Trans. Microwave Theory Tech.,* vol. MTT-27, no. 4, pp. 987–993, Apr. 1979.

[6] R. Gillon, J. P. Raskin, D. Vanhoenacker, and J. P. Colinge, "Determining the reference impedance of on-wafer TLR calibrations on lossy substrates," in *26th EuMC,* Prague, Czech Republic, Sept. 9–12, pp. 170–173.